Supporting Information

Redox-Switchable Pickering Emulsion Stabilized by Hexaniobate-based Ionic Liquid for Oxidation Catalysis

Wei Lu, Jing Dong,* Di Zhang, Peng Lei, Yingnan Chi* and Changwen Hu

Table of Contents

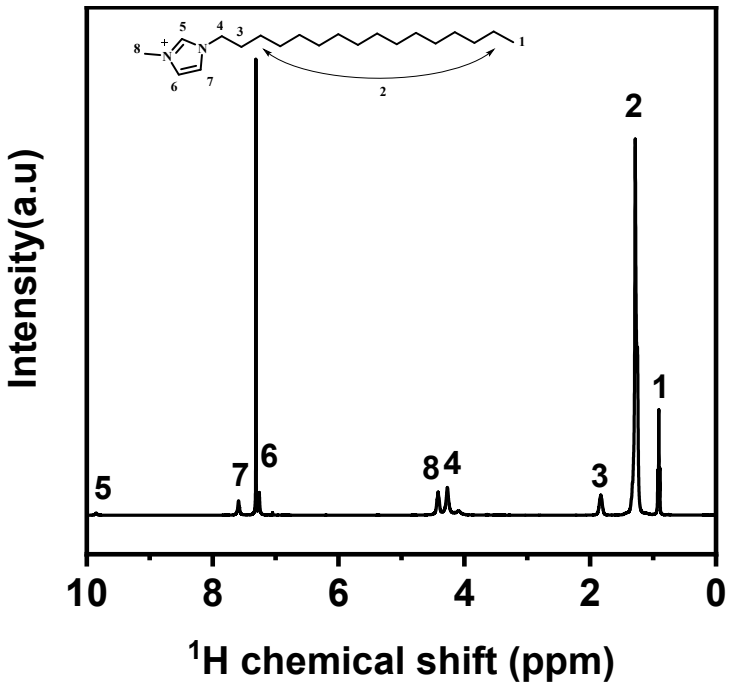

Figure S1. ^{1}H NMR spectra of $[C_{16}MIM]Nb_6$ in $CDCl_3$. ^{1}H NMR (400 MHz, $CDCl_3$) of $[C_{16}MIM]Nb_6$, δ 9.96 (s, 1H), 7.49 (s, 1H), 7.22 (s, 1H), 4.41 (s, 2H), 4.24 (s, 3H), 1.82 (s, 2H), 1.23 (d, J = 12.5 Hz, 26H), 0.87 (t, J = 6.8 Hz, 3H).

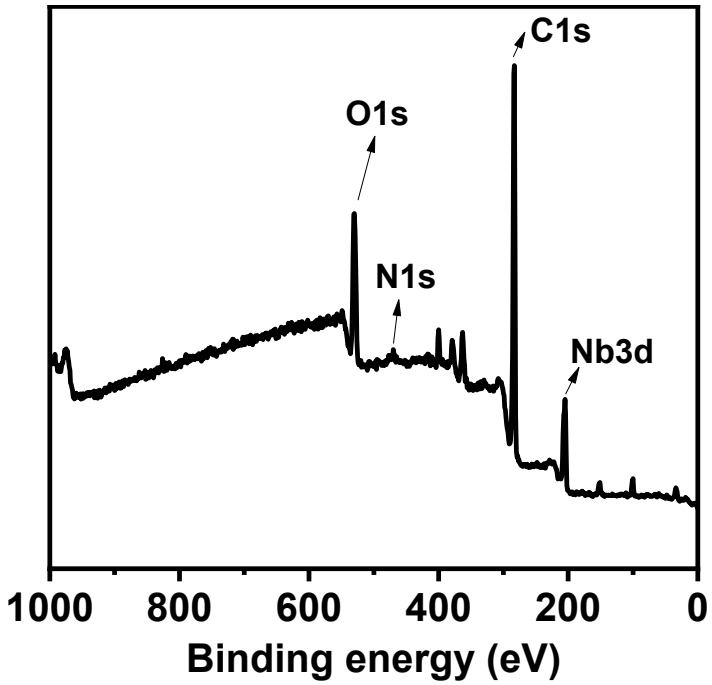

Figure S2. XPS survey of $[C_{16}MIM]Nb_6$.

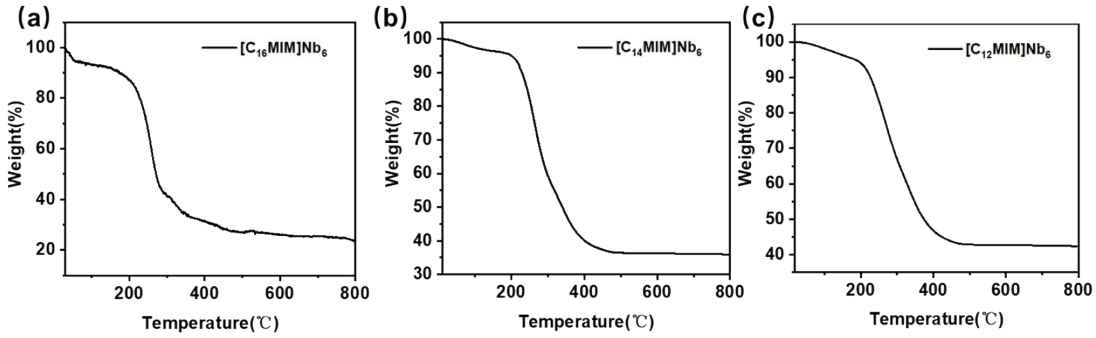

Figure S3. Thermogravimetric analyses of $[C_{16}MIM]Nb_6$ (a), $[C_{14}MIM]Nb_6$ (b), and $[C_{12}MIM]Nb_6$ (c). For $[C_{16}MIM]Nb_6$, the first weight loss of 8 % between 24-153 °C can be ascribed to the loss of crystallographic water molecules. The second step weight loss of 65.4 % in the range of 153-549 °C is attributed to the decomposition of 1-hexadecyl-3-methylimidazolium cation. For $[C_{14}MIM]Nb_6$, the first weight loss of 4.0 % in the range of 20-172 °C is due to the removal of lattice water molecules. The second step weight loss of 59.6 % at 172-509 °C is attributed to the decomposition of 1-tetradecyl-3-methylimidazolium cation. For $[C_{12}MIM]Nb_6$, the first weight loss of 4.7 % between 20-178 °C is attributed to the loss of water molecules. The second step weight loss of 52.4 % in the range of 178-493 °C can be ascribed to the decomposition of 1-dodecyl-3-methylimidazolium cations.

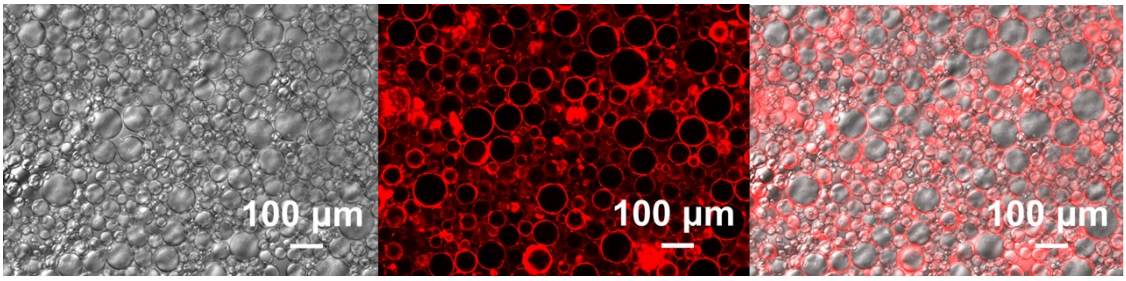

Figure S4. Confocal microscopy images of Pickering emulsion formed by H_2O_2-treated $[C_{16}MIM]Nb_6$, where the oil phase was stained by 0.01 wt% Nile Red. (left: light-field, middle: dark-field, right: superposed field)

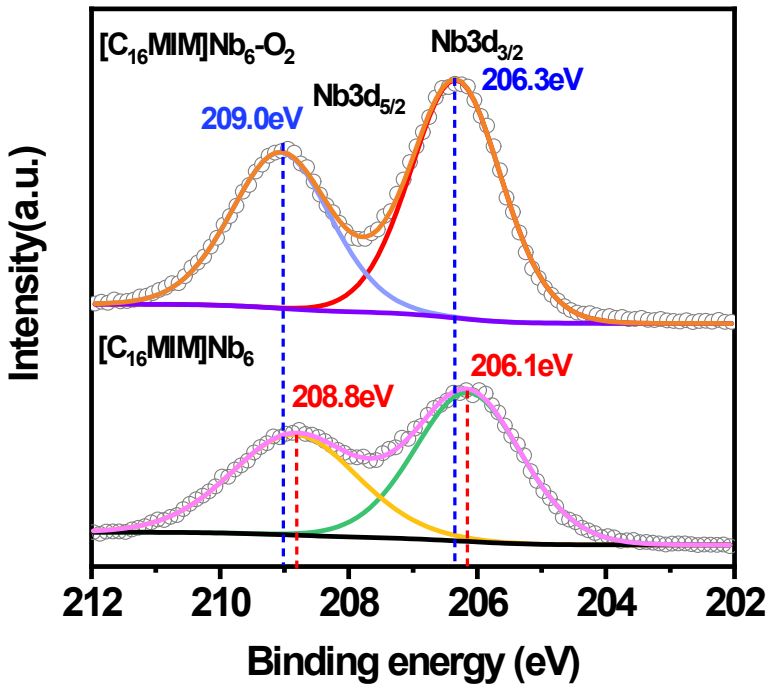

Figure S5. XPS spectra of $[C_{16}MIM]Nb_6$ and $[C_{16}MIM]Nb_6$-O_2.

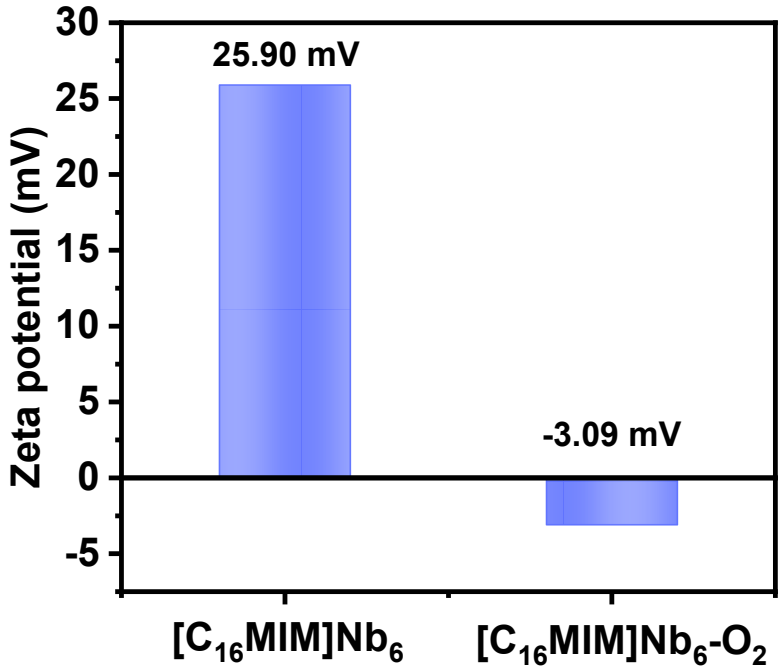

Figure S6. Zeta potential of $[C_{16}MIM]Nb_6$ and $[C_{16}MIM]Nb_6$-O_2.

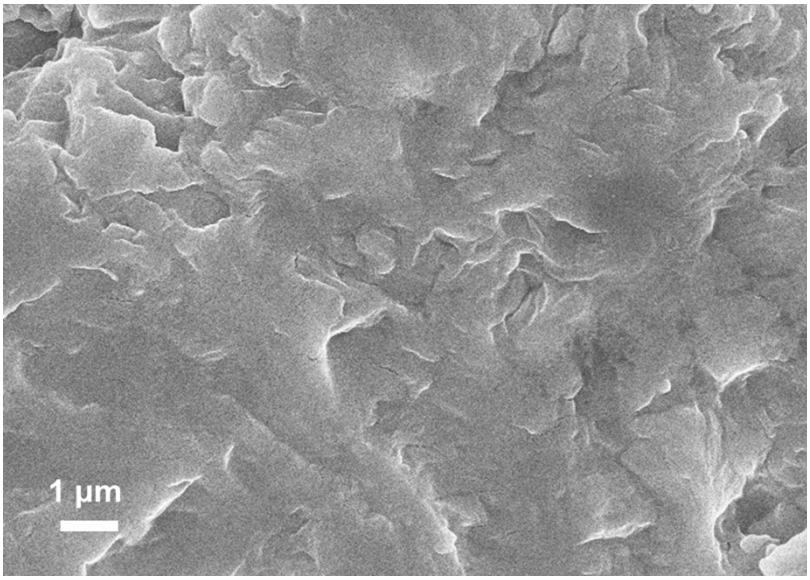

Figure S7. SEM image of $[C_{16}MIM]Nb_6$.

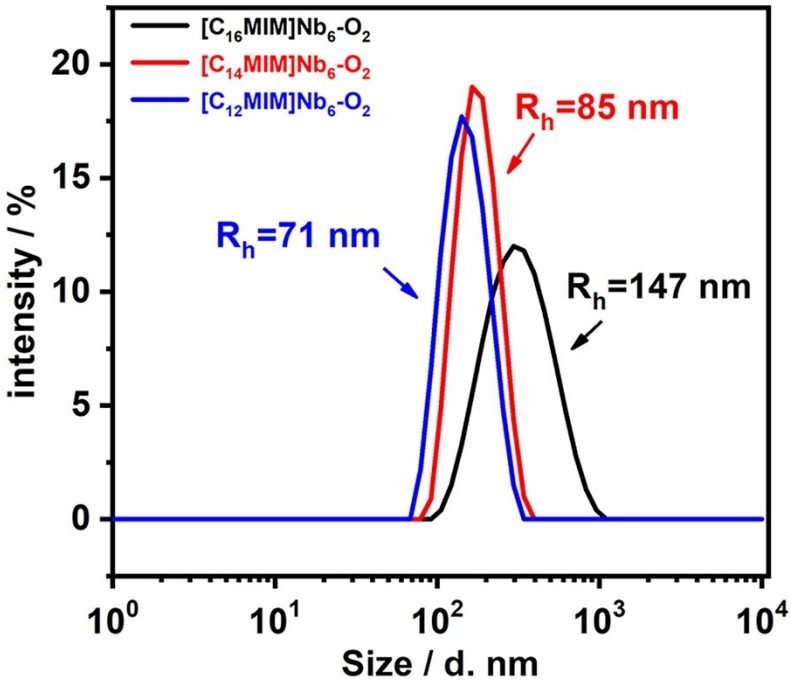

Figure S8. Particle size of the three amphiphilic hexaniobate-based ionic liquids measured by DLS**.**

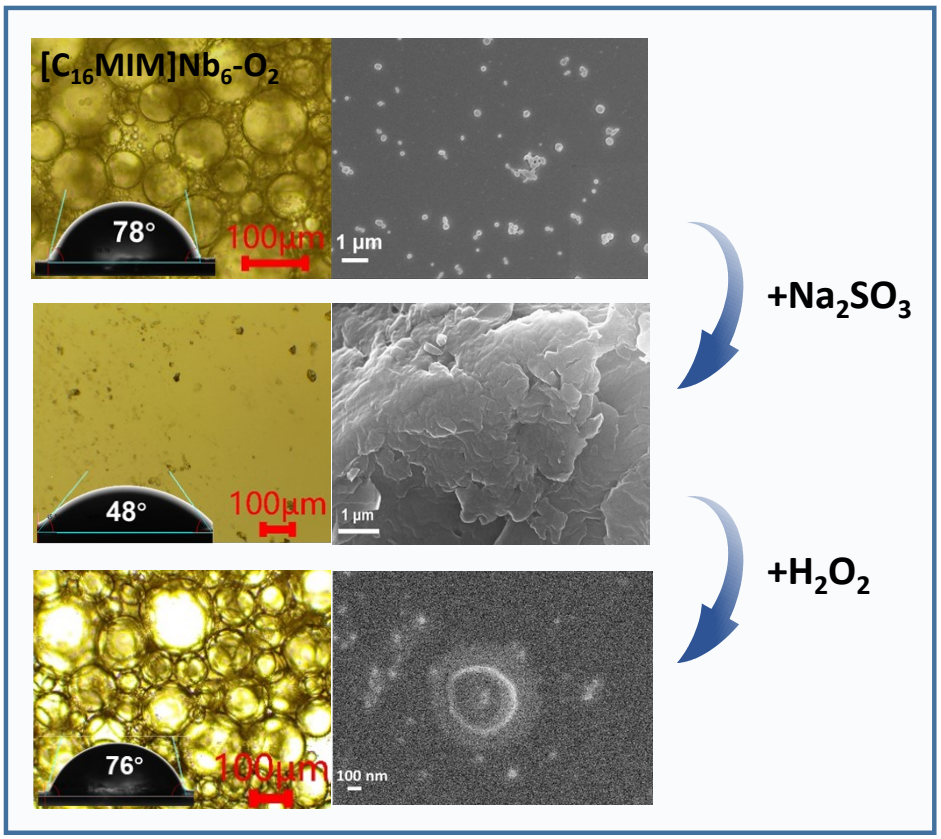

Figure S9. Optical micrographs of the Pickering emulsion stabilized by $[C_{16}MIM]Nb_6$-O_2 (left) and SEM images of the emulsifiers (right).

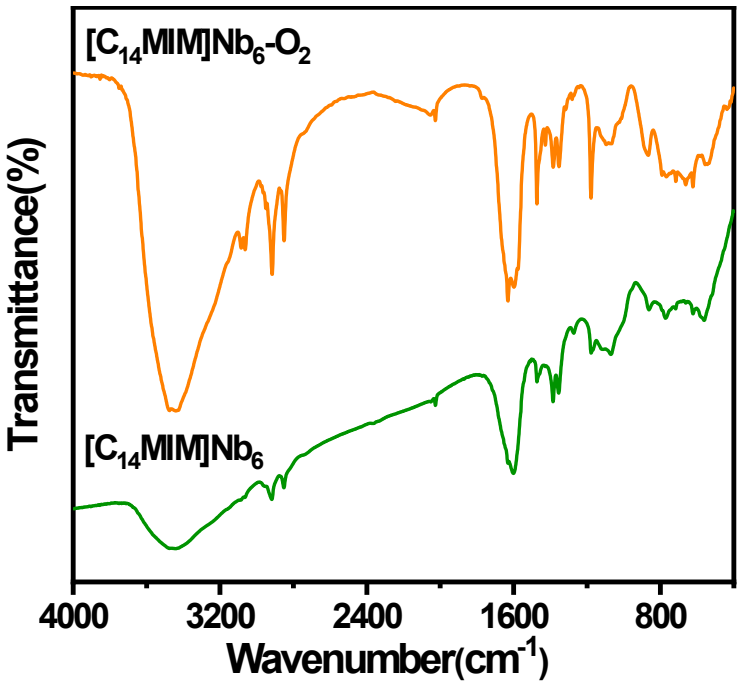

Figure S10. FT-IR spectra of $[C_{14}MIM]Nb_6$ and $[C_{14}MIM]Nb_6$-O_2.

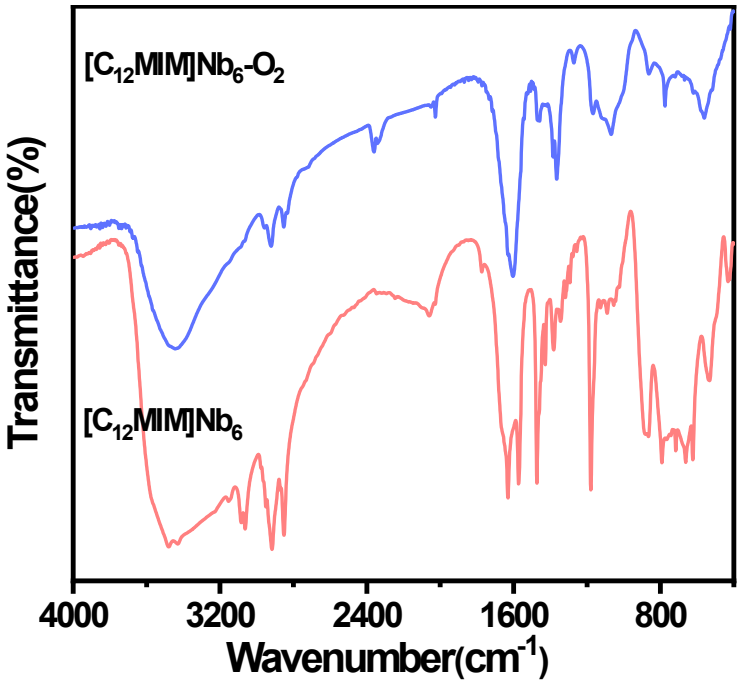

Figure S11. FT-IR spectra of $[C_{12}MIM]Nb_6$ and $[C_{12}MIM]Nb_6$-O_2.

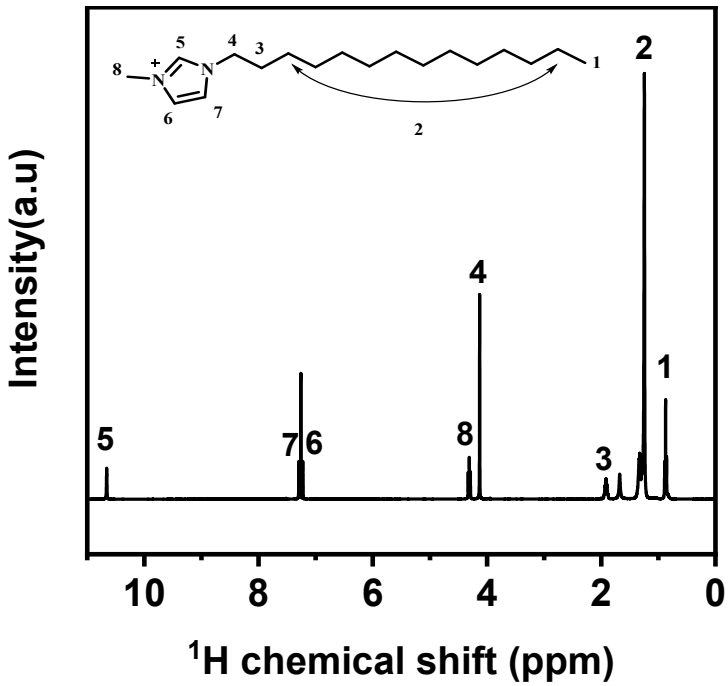

Figure S12. ^{1}H NMR spectra of $[C_{14}MIM]Nb_6$ in $CDCl_3$. ^{1}H NMR (400 MHz, $CDCl_3$) of $[C_{14}MIM]Nb_6$, δ 10.66 (s, 1H), 7.29 (s, 1H), 7.23 (s, 1H), 4.31 (t, J = 7.5 Hz, 2H), 4.13 (s, 3H), 1.91 (dd, J = 14.1, 7.1 Hz, 2H), 1.40 – 1.15 (m, 22H), 0.91 – 0.82 (m, 3H).

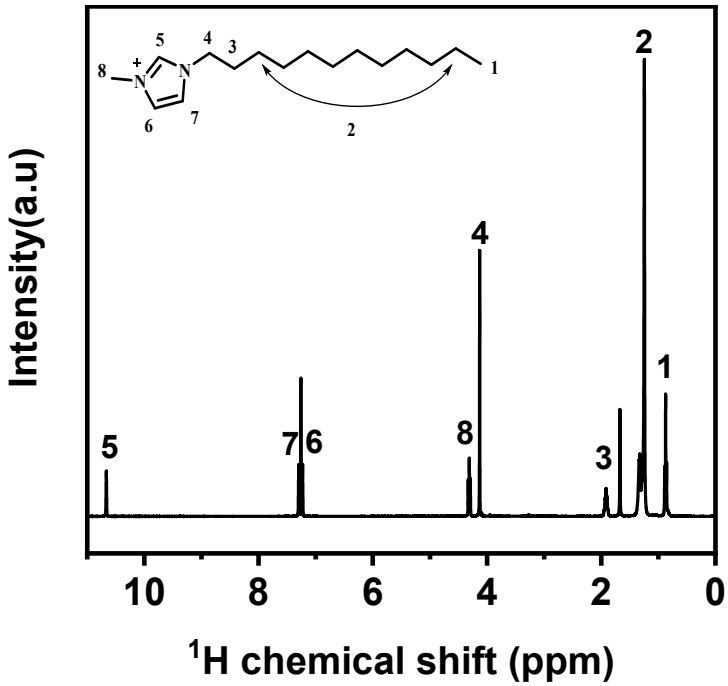

Figure S13. ^{1}H NMR spectra of $[C_{12}MIM]Nb_6$ in $CDCl_3$. ^{1}H NMR (400 MHz, $CDCl_3$) of $[C_{12}MIM]Nb_6$, δ 10.67 (s, 1H), 7.30 (s, 1H), 7.23 (s, 1H), 4.31 (t, J = 7.5 Hz, 2H), 4.13 (s, 3H), 1.91 (dd, J = 14.3, 7.3 Hz, 2H), 1.39 – 1.20 (m, 18H), 0.91 – 0.82 (m, 3H).

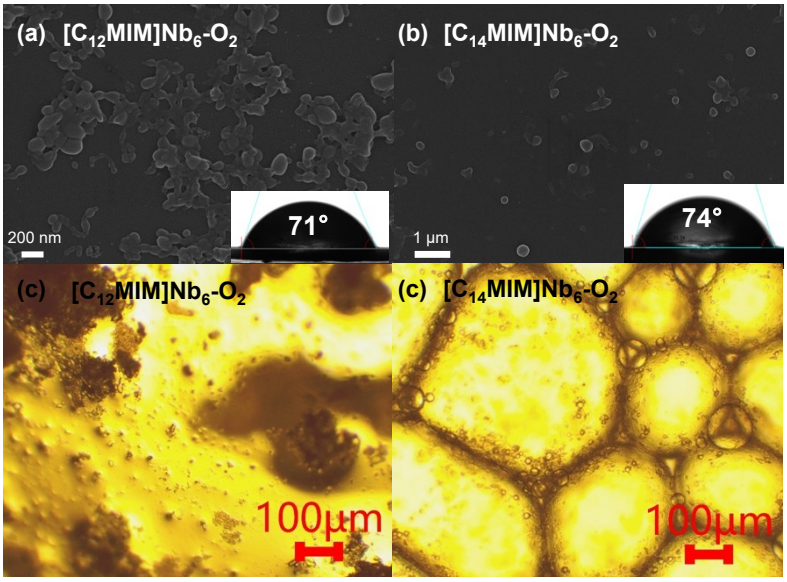

Figure S14. (a) SEM image of $[C_{12}MIM]Nb_6$-O_2 (inset: water contact angle); (b) SEM image of $[C_{14}MIM]Nb_6$-O_2 (inset: water contact angle); (c) microscope photograph of the oil-water system containing $[C_{12}MIM]Nb_6$-O_2; (d) microscope photograph of Pickering emulsion stabilized by $[C_{14}MIM]Nb_6$-O_2.

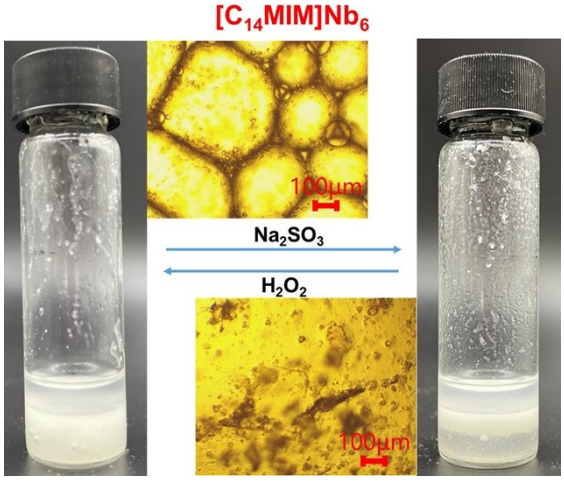

Figure S15. The optical micrographs of the reversible redox-triggered emulsification and demulsification of the Pickering emulsion containing $[C_{14}MIM]Nb_6$-O_2.

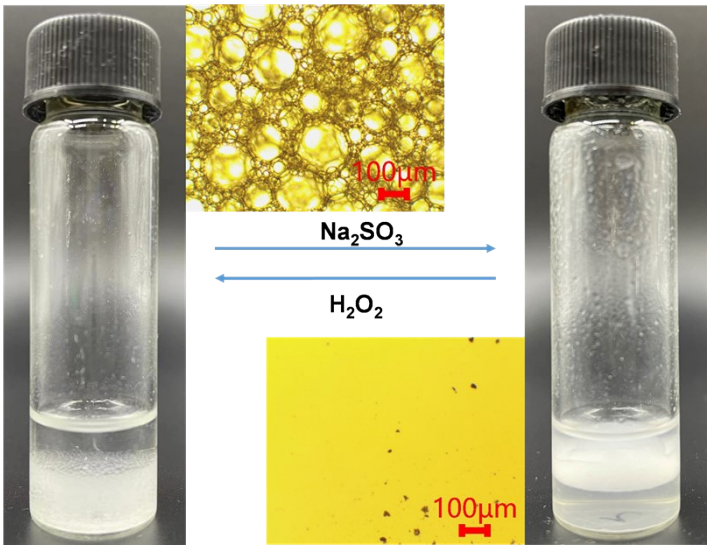

Figure S16. Optical micrographs of isooctane-water emulsion system stabilized with $[C_{16}MIM]Nb_6\text{-}O_2$.

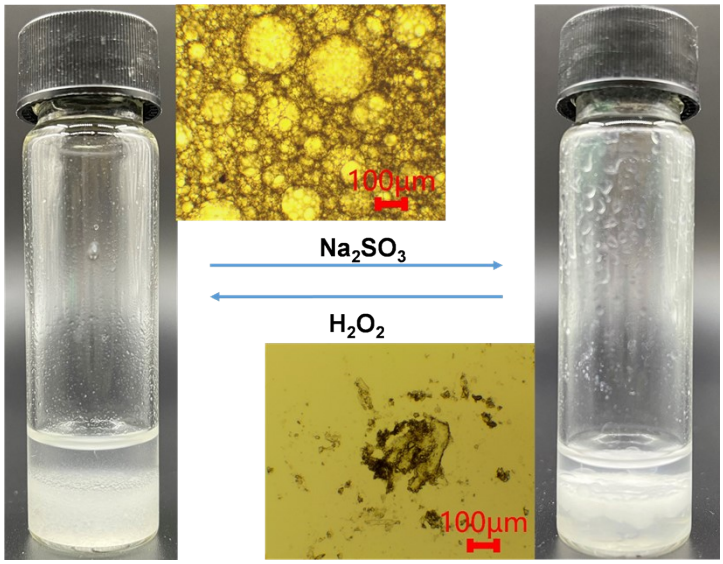

Figure S17. Optical micrographs of *n*-heptane-water emulsion system stabilized with $[C_{16}MIM]Nb_6\text{-}O_2$.

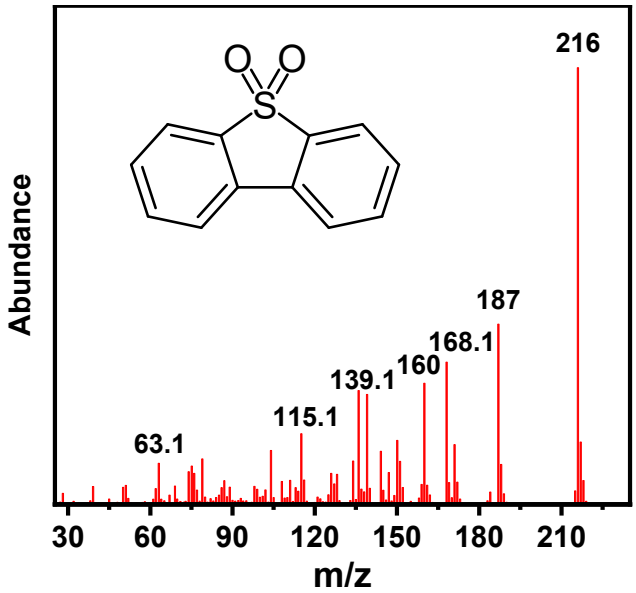

Figure S18. The GC-MS spectrum of the oxidation product of DBT.

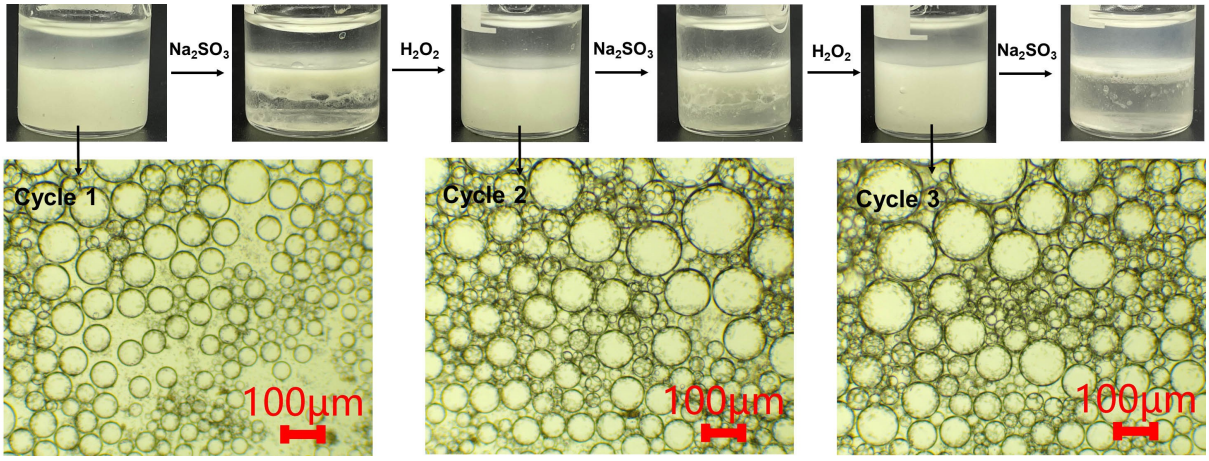

Figure S19. The optical micrographs of emulsion droplets in the recycle test.

Figure S20. Photographs of redox-responsive Pickering emulsion.

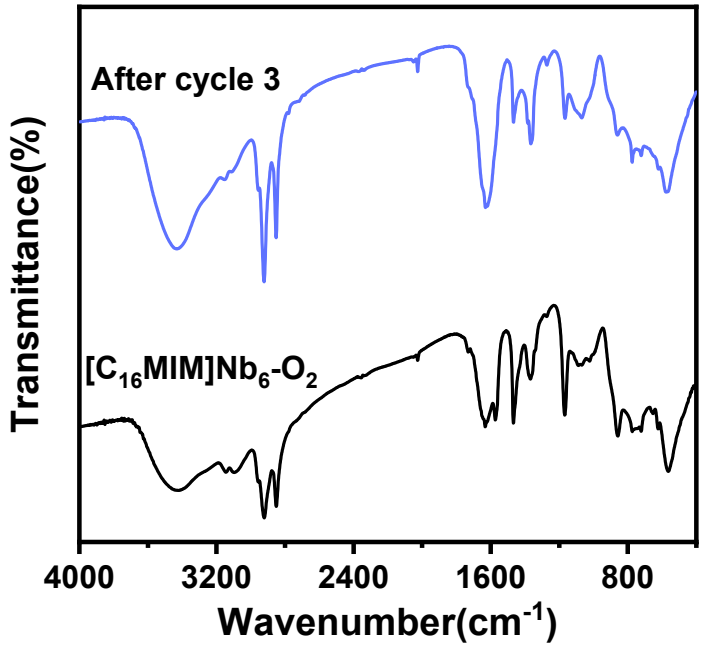

Figure S21. FT-IR spectra of $[C_{16}MIM]Nb_6$-O_2 before and after the catalytic reaction.

Table S1 The elemental analysis of $[C_nMIM]Nb_6$.

Sample	C (wt%)	H (wt%)	N (wt%)	Nb (wt%)	Molecular formula
$[C_{16}MIM]Nb_6$	46.75	8.21	5.44	13.42	$(C_{20}H_{39}N_2)_8Nb_6O_{19}\cdot 16H_2O$
$[C_{14}MIM]Nb_6$	42.40	7.34	5.39	21.92	$(C_{18}H_{35}N_2)_5H_3Nb_6O_{19}\cdot 5H_2O$
$[C_{12}MIM]Nb_6$	38.69	6.41	5.56	25.84	$(C_{16}H_{31}N_2)_4H_4Nb_6O_{19}\cdot 5H_2O$

Table S2. Oxidative desulfurization of DBT and other S-containing compounds in the Pickering emulsion system.

Entry	Substrate	Time	Conversion (%)
1[a]	DBT	40 min	>99
2[a]	BT	60 min	>99
3[a]	DT	120 min	>99
4[b]	4,6-DMDBT	12 h	70

[a] Reaction conditions: $[C_{16}MIM]Nb_6$-O_2 (0.003 mmol), H_2O_2 (0.3 mmol), n-octane (1 mL) containing substrate (800 ppm), H_2O (1 mL), 40 °C . [b] $[C_{16}MIM]Nb_6$-O_2 (0.003 mmol), H_2O_2 (1 mmol), n-octane (1 mL) containing substrate (800 ppm), H_2O (1 mL), 60 °C.

Table S3 Comparison of stimuli-responsive emulsion systems.

Emulsifier	Stimulus response type	Demulsification			Stimulus response site	Catalytic application	Ref.
		Method	Temp. /ºC	Time			
$[C_{16}MIM]Nb_6$-O_2	redox	adding Na_2SO_3	r.t.	40 s	heterogeneous	yes	This work
Ferrocene surfactant ($FcCOC_{10}N$)/SiO_2	redox	0.8V electrical oxidation	-	2 h	homogeneous	no	1
C_{10}–Se–C_{10}·$(COONa)_2$/Al_2O_3	redox	adding H_2O_2	r.t.	50 s	homogeneous	no	2
$C_{16}H_{34}N_2$@SiO_2	CO_2-N_2	bubbling N_2	65	80 min	heterogeneous	no	3
Triethylenetetramine-functionalized MOFs	CO_2-N_2	bubbling N_2	50	30 min	heterogeneous	yes	4
N-alkylimidazoles bicarbonates $[C_nIM]^+HCO_3^-$/SiO_2	CO_2-N_2	bubbling N_2	25	40 min	homogeneous	no	5
Fe_3O_4@SiO_2@P(TMA-DEA)	CO_2-N_2	bubbling CO_2	r.t.	-	heterogeneous	yes	6
$(MeO)_3SiCH_2CH_2CH_2(NHCH_2CH_2)_2NH_2$@$(MeO)_3Si(CH_2)_7CH_3)$@$SiO_2$	pH	adding HCl	r.t.	3-5 min	heterogeneous	no	7
Lipase AYS@magnetic hollow mesoporous carbon nanospheres (AYS@MHMCS)	magnetism	magnetic field	-	15 min	heterogeneous	yes	8
Pd-SiO_2/azobenzene	light	UV irradiation	25	30 min	homogeneous	yes	9
Grafted silanes on TiO_2 nanoparticles	light	UV irradiation	-	36 h	heterogeneous	no	10

"-": not mentioned

Table S4 Comparison of polyoxometalate-based emulsion catalysts in the oxidative desulfurization of DBT.

Catalyst	Temp. (°C)	Extraction agent	System	Time	Conv. (%)	Reference
$[C_{16}MIM]Nb_6$-O_2	40	H_2O	**stimuli-responsive emulsion**	40 min	>99	This work
Organic-functionalized V_6O_{19}	40	H_2O	emulsion	80 min	98	11
$[C_{16}H_{33}N(CH_3)_3]_{11}P_2W_{13}V_5O_{64}$	60	IL	emulsion	60 min	98	12
$[BMIM]_4SiW_{12}O_{40}$ -based Janus nanosheets	60	IL	emulsion	90 min	>99	13
$PW_{12}O_{40}$/P[tVPB-VPx]	50	methanol	emulsion	2 h	99	14
C-SiO_2-$PW_{12}O_{40}$	50	acetonitrile	emulsion	2 h	>99	15
$[(C_nH_{2n+1})_3NCH_3]_2W_6O_{19}$	60	IL	emulsion	20 min	98	16
$[C_{16}H_{33}N(CH_3)_3]_{11}P_2W_{13}V_5O_{64}$	70	IL	emulsion	45 min	100	17
SiO_2@C-dots/PW_{12}	50	acetonitrile	biphase	3 h	100	18
PMo_{12}/BzPN-SiO_2	60	H_2O	biphase	3 h	100	19

Reference

1 S. Yu, D. Zhang, J. Jiang and W. Xia, *ACS Sustainable Chem. Eng.*, 2019, **7**, 15904-15912.

2 S. Yu, H. Zhang, J. Jiang, Z. Cui, W. Xia and B. P. Binks, *Green Chem.*, 2020, **22**, 5470-5475.

3 J. Jiang, Y. Zhu, Z. Cui and B. P. Binks, *Angew. Chem. Int. Ed.*, 2013, **52**, 12373-12376.

4 Y. Shi, D. Xiong, Z. Li, H. Wang, J. Qiu, H. Zhang and J. Wang, *ACS Appl. Mater. Interfaces*, 2020, **12**, 53385-53393.

5 Y. Shi, D. Xiong, Y. Chen, H. Wang and J. Wang, *J. Mol. Liq.*, 2019, **274**, 239-245.

6 J. Tang, X. Zhou, S. Cao, L. Zhu, L. Xi and J. Wang, *ACS Appl. Mater. Interfaces*, 2019, **11**, 16156-16163.

7 J. Huang and H. Yang, *Chem. Commun.*, 2015, **51**, 7333-7336.

8 T. Yang, Y. Zhang, J. Wang, F. Huang and M. Zheng, *ACS Sustainable Chem. Eng.*, 2021, **9**, 12070-12078.

9 Z. Li, Y. Shi, A. Zhu, Y. Zhao, H. Wang, B. P. Binks and J. Wang, *Angew. Chem. Int. Ed.*, 2021, **60**, 3928-3933.

10 Q. Zhang, R. X. Bai, T. Guo and T. Meng, *ACS Appl. Mater. Interfaces*, 2015, **7**, 18240-18246.

11 Y. Ding, W. Zhu, H. Li, W. Jiang, M. Zhang, Y. Duan and Y. Chang, *Green Chem.*, 2011, **13**, 1210-1216.

12 P. Yin, J. Wang, Z. Xiao, P. Wu, Y. Wei and T. Liu, *Chem. Eur. J.*, 2012, **18**, 9174-9178.

13 D. Julião, A. C. Gomes, M. Pillinger, R. Valença, J. C. Ribeiro, B. D. Castro, I. S. Gonçalves, L. C. Silva and S. S. Balula, *Eur. J. Inorg. Chem.*, 2016, DOI: 10.1002/ejic.201600442, 5114-5122.

14 F. Banisharif, M. R. Dehghani and J. M. Campos-Martin, *Energy Fuels*, 2017, **31**, 5419-5427.

15 F. Banisharif, M. R. Dehghani, M. Capel-Sánchez and J. M. Campos-Martin, *Ind. Eng. Chem. Res*, 2017, **56**, 3839-3852.

16 M. Craven, X. Dong, C. Kunstmann-Olsen, E. F. Kozhevnikova, F. Blanc, A. Steiner and I. V. Kozhevnikov, *Appl. Catal. B Environ.*, 2018, **231**, 82-91.

17 Y. Q. Zhang and R. Wang, *Appl. Catal. B Environ.*, 2018, **234**, 247-259.

18 S. Y. Dou and R. Wang, *Chem. Eng. J.*, 2019, **369**, 64-76.

19 R. Xia, W. Lv, K. Zhao, S. Ma, J. Hu, H. Wang and H. Liu, *Langmuir*, 2019, **35**, 3963-3971.